

# Euclid weak lensing simulations + calibration

Tim Schrabbach (AifA Bonn)

ISSI meeting, Beijing, Nov. 5th, 2019

Euclid (Artist impression, ESA)

# Outline

- 1) Introduction
- 2) Euclid shape measurement methods: Moments ML
- 3) Using HST data as inputs
- 4) Impact of faint galaxies
- 5) Simulating cluster environments
- 6) OU-SIM simulations
- 7) Summary

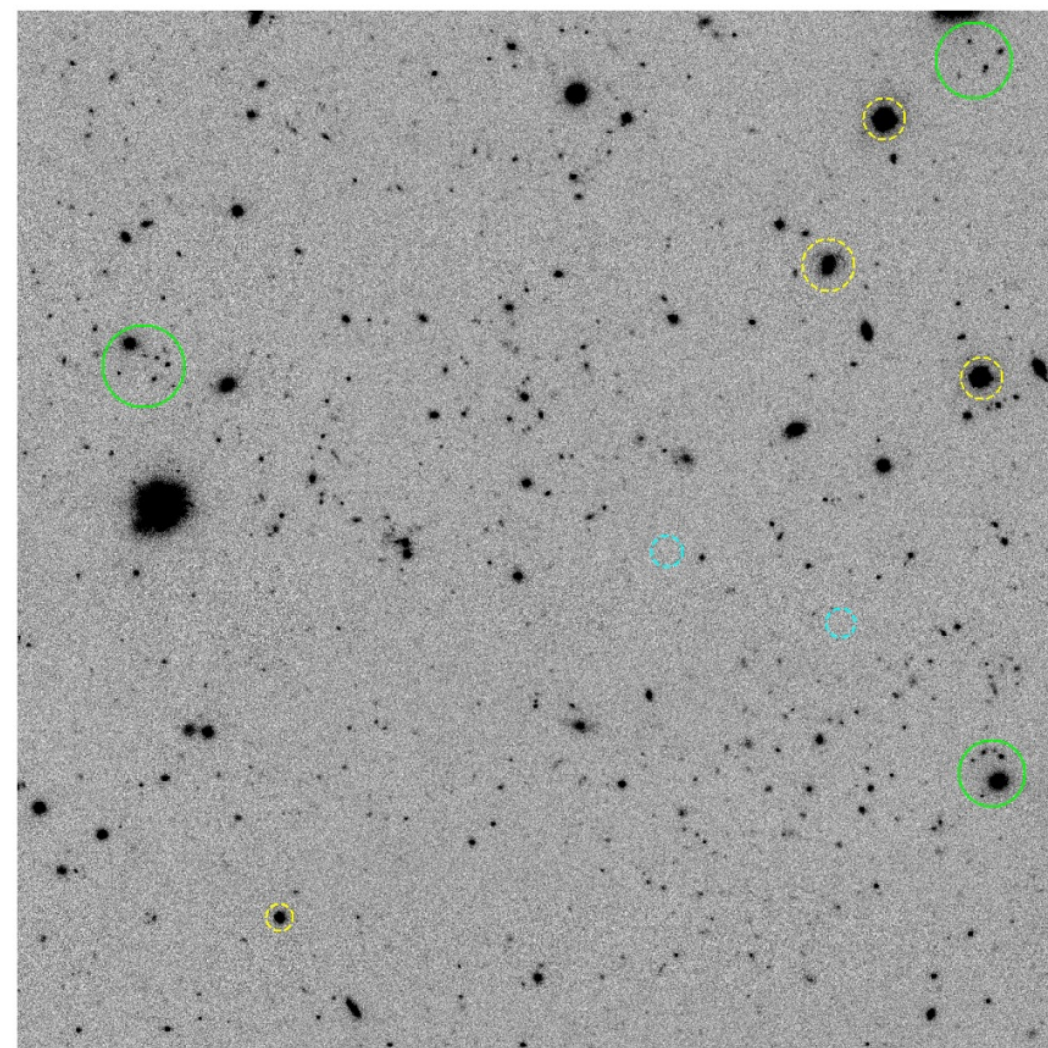
# 1. Introduction

Weak lensing image simulations are needed to:

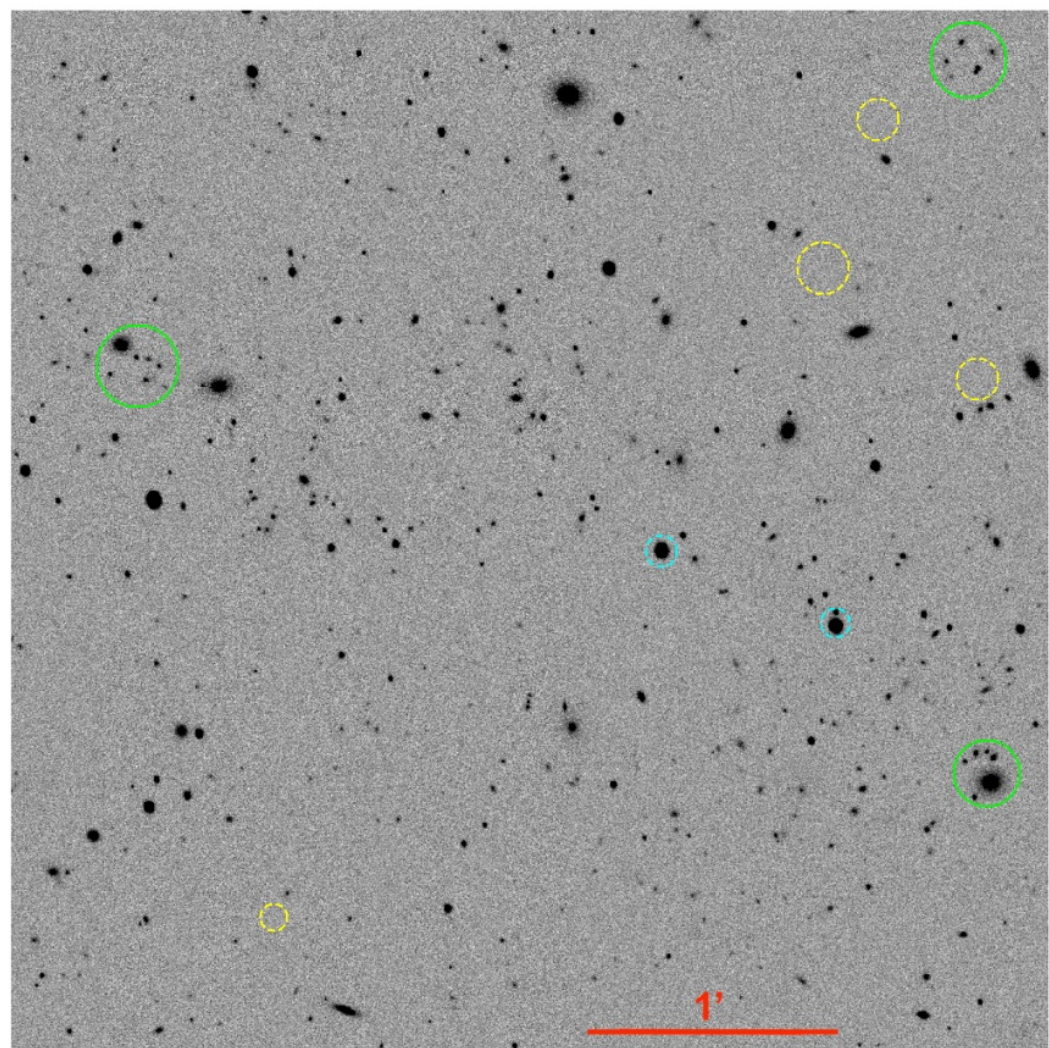
- 1) Calibrate shape measurement methods
- 2) Verify their accuracy & correct for residual biases if needed

Need to make sure that:

- The simulations resemble the real data with sufficient accuracy
- What does “sufficient accuracy” mean?
- Depends on the sensitivity of the biases of a particular shape measurement on the details of the simulation → Needs to be measured
- Useful: Introduce metrics that compare the statistical properties of the simulation and the sky data, or try to emulate existing sky data



KiDS



Emulation

From Kannawadi et al. (2019), emulating KiDS-like observations of the COSMOS field based on HST galaxy measurements

## 2. Overview Euclid OU-SHE shape measurement methods

Shape measurement methods currently developed by OU-SHE:

- 1) **lensMC** (UK-led: Giuseppe Congedo, Niraj Welikala)
- 2) **MomentsML** (DE-led: Malte Tewes)
- 3) **Bayesian Fourier Domain** (BFD) method (US-led: Kathleen Eckert, Gary Bernstein)

For Euclid we need to reach an accuracy one order of magnitude higher than current WL surveys:

- Originally had to go back to the drawing board
- Continuous method evaluation → Changed from FDNT to MomentsML
- Aided by WL-SWG efforts (e.g. test of MetaCal for Euclid)

# Weak-lensing shear measurement with machine learning

## Teaching artificial neural networks about feature noise

M. Tewes<sup>1</sup>, T. Kuntzer<sup>2</sup>, R. Nakajima<sup>1</sup>, F. Courbin<sup>2</sup>, H. Hildebrandt<sup>1</sup>, and T. Schrabback<sup>1</sup>

<sup>1</sup> Argelander-Institut für Astronomie, Auf dem Hügel 71, D-53121 Bonn, Germany

<sup>2</sup> Institute of Physics, Laboratory of Astrophysics, Ecole Polytechnique Fédérale de Lausanne (EPFL), Observatoire de Sauverny, CH-1290 Versoix, Switzerland

February 1, 2019

### ABSTRACT

Cosmic shear, that is weak gravitational lensing by the large-scale matter structure of the Universe, is a primary cosmological probe for several present and upcoming surveys investigating dark matter and dark energy, such as *Euclid* or WFIRST. The probe requires an extremely accurate measurement of the shapes of millions of galaxies based on imaging data. Crucially, the shear measurement must address and compensate for a range of interwoven nuisance effects related to the instrument optics and detector, noise in the images, unknown galaxy morphologies, colors, blending of sources, and selection effects. This paper explores the use of supervised machine learning as a tool to solve this inverse problem. We present a simple architecture that learns to regress shear point estimates and weights via shallow artificial neural networks. The networks are trained on simulations of the forward observing process, and take combinations of moments of the galaxy images as inputs. A challenging peculiarity of the shear measurement task, in terms of machine learning applications, is the combination of the noisiness of the input features and the requirements on the statistical accuracy of the inverse regression. To address this issue, the proposed training algorithm minimizes bias over multiple realizations of individual source galaxies, reducing the sensitivity to properties of the overall sample of source galaxies. Importantly, an observational selection function of these source galaxies can be straightforwardly taken into account via the weights. We first introduce key aspects of our approach using toy-model simulations, and then demonstrate its potential on images mimicking *Euclid* data. Finally, we analyze images from the GREAT3 challenge, obtaining competitively low multiplicative and additive shear biases despite the use of a simple training set. We conclude that the further development of suited machine learning approaches is of high interest to meet the stringent requirements on the shear measurement in current and future surveys. We make a demonstration implementation of our technique publicly available.

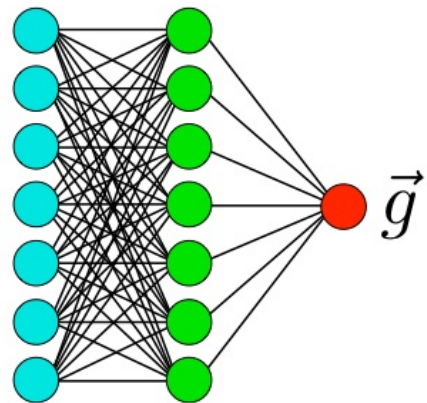
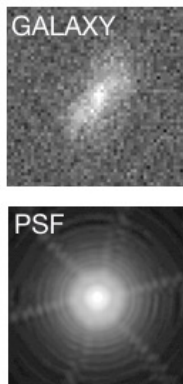
**Key words.** methods: data analysis – gravitational lensing: weak – cosmological parameters

### 1. Introduction

Images of distant galaxies appear slightly distorted, typically at the percent level, as light bundles reaching the observer are differentially deflected owing to gravitational lensing by massive structures along the line of sight. Since galaxies come in a variety of intrinsic shapes, inclinations, and orientations, these weak distortions are not identifiable on individual sources. In this sense, galaxies give us only a very noisy view of the distortion field. However, despite this intrinsic “shape noise”, the weak lensing (WL) effect imprints spatial correlations on the apparent galaxy shapes. Observing these spatial correlations, ideally as a function of redshift, allows us to infer properties of the large-scale matter structure of the Universe, and how this structure has

views on the field, with a particular focus on the analysis methods to interpret the data from wide field surveys.

The statistical uncertainty of cosmic shear measurements, which is related to the finite number of galaxies probing the shear field, decreases with the increasing sky coverage and depth of the surveys. To make full use of large surveys, the accuracy of the data analysis methods must therefore be high enough to avoid that systematic errors dominate the error-budget of the cosmological parameter inference (Refregier 2003). For *Euclid*, surveying 15 000 square degrees of extra-galactic sky, the resulting accuracy requirements are unprecedented. These requirements flow down, on the observational side, to (1) the determination of redshifts and (2) the measurement of shear. The cosmology



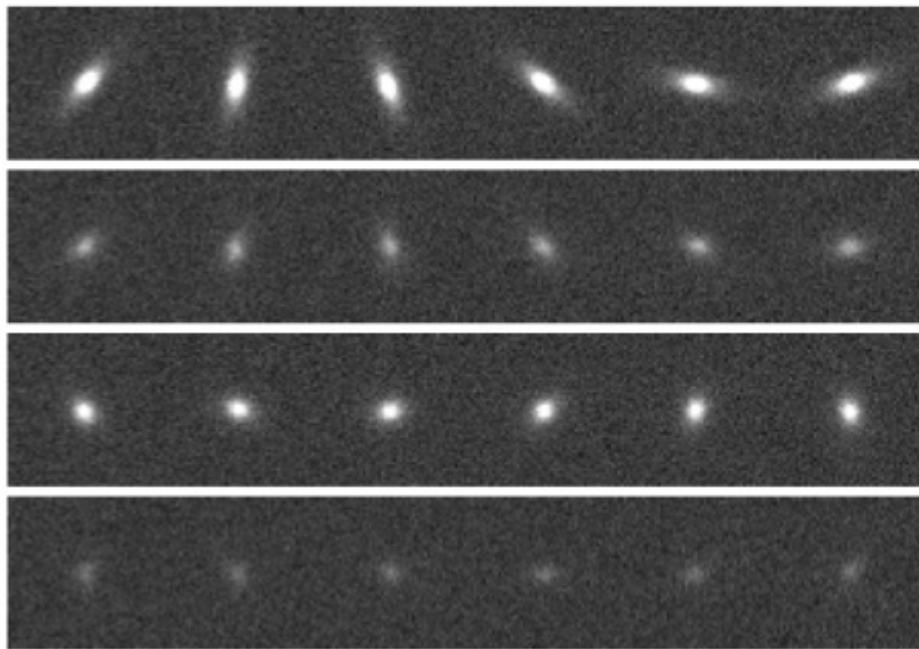
Xiv:1807.02120v2 [astro-ph.CO] 30 Jan 2019

# Current algorithm has 2 training steps & datasets:

## 1) Train shear point estimates, aiming at low sensitivity

Realizations differ in true orientation (shape noise cancellation), in noise, and sub-pixel position.

Cases differ in shear, galaxies, and PSFs.



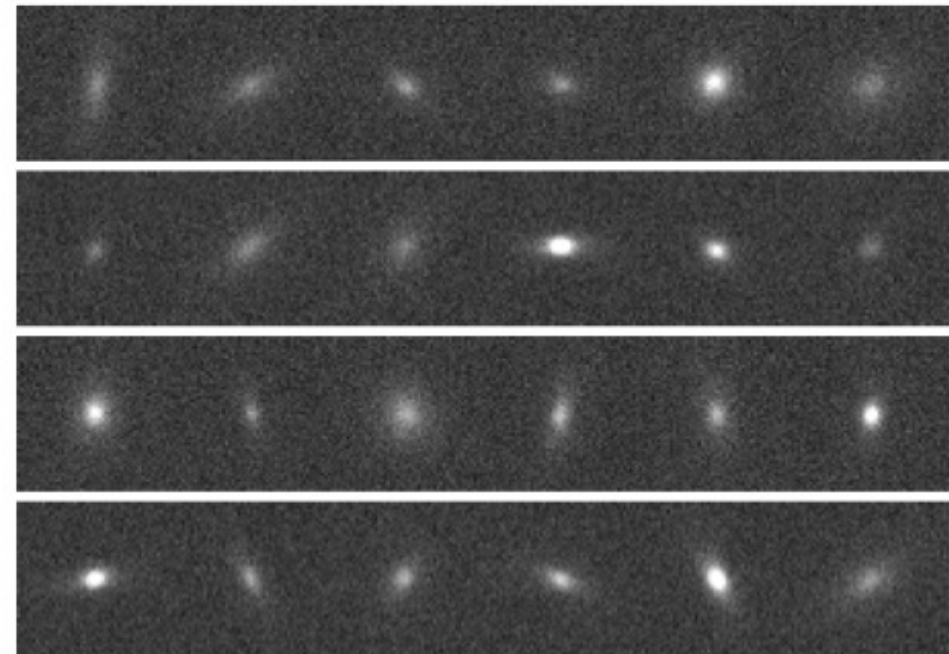
Cost functions:

$$C_{\text{MSB}}(\mathbf{p}) \doteq \frac{1}{n_{\text{case}}} \sum_{k=1}^{n_{\text{case}}} \left( \frac{1}{n_{\text{rea}}} \sum_{i=1}^{n_{\text{rea}}} \hat{g}_{ik}(\mathbf{p}) - g_{\text{true},k} \right)^2$$

## 2) Train shear *weights*, given a source population and **selection function**

Realizations differ in galaxies, noise, and sub-pixel position.

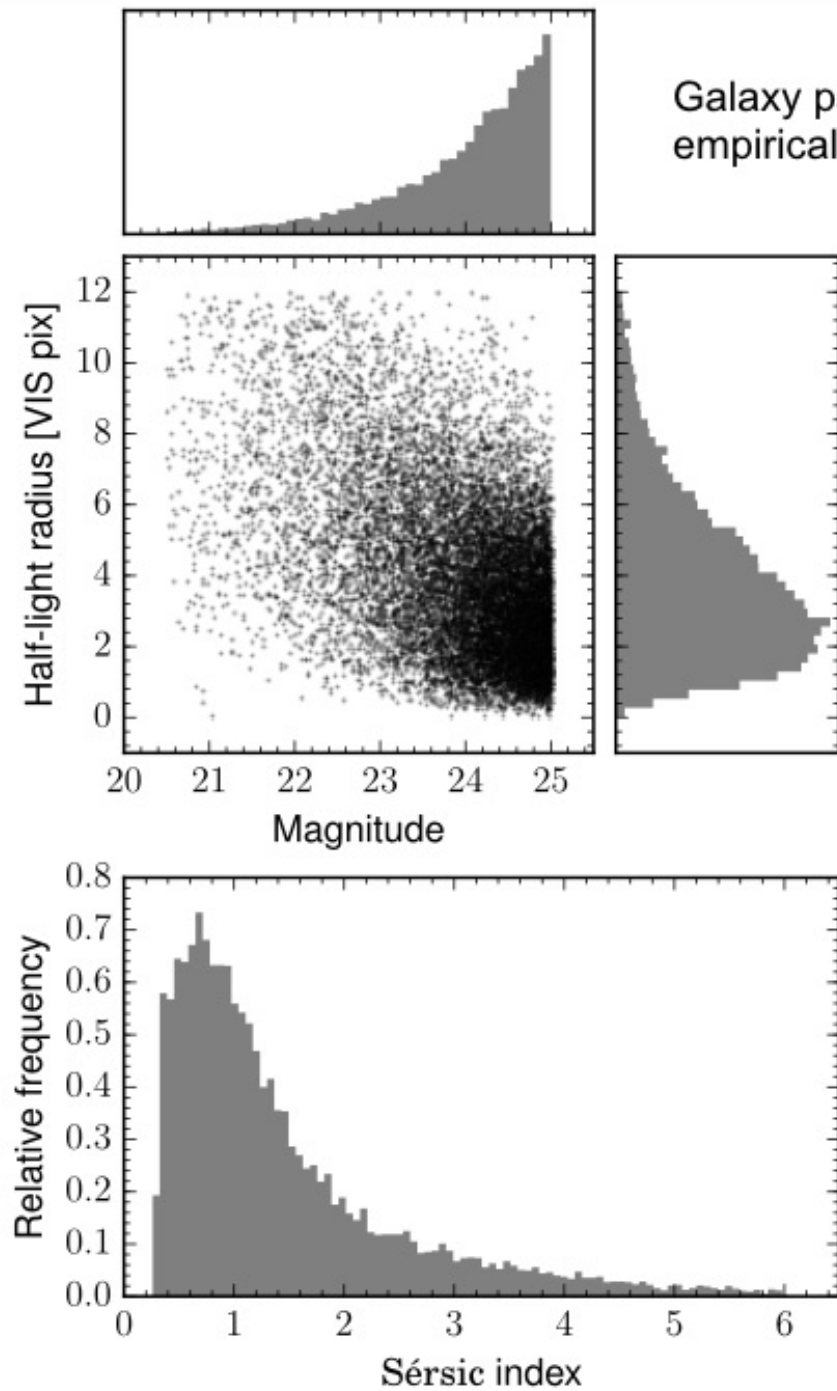
Cases differ in shear and PSFs.



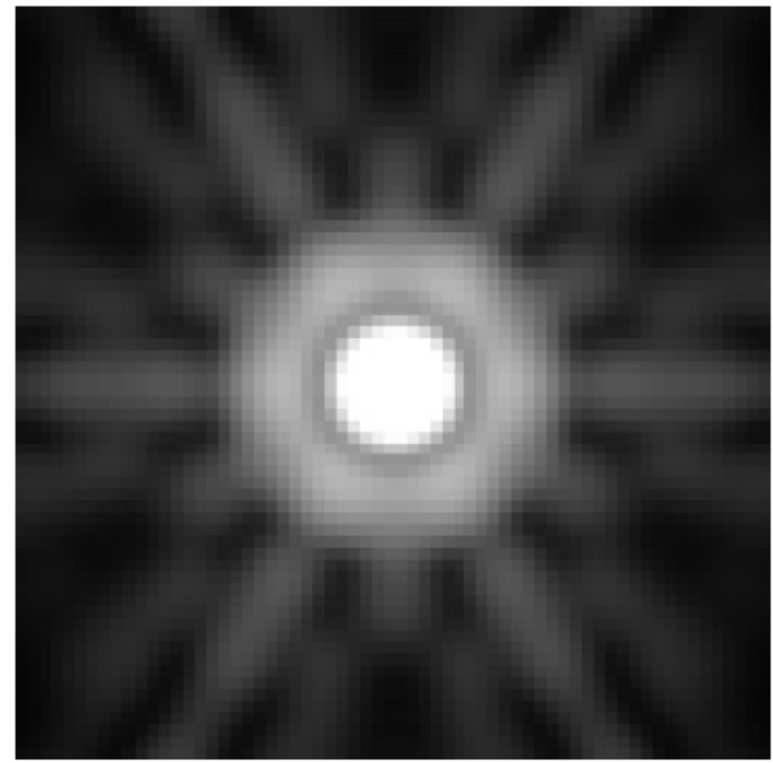
$$C_{\text{MSWB}}(\mathbf{p}) \doteq \frac{1}{n_{\text{case}}} \sum_{k=1}^{n_{\text{case}}} \left( \frac{\sum_{i=1}^{n_{\text{rea}}} \hat{g}_{ik} \cdot w_{ik}(\mathbf{p})}{\sum_{i=1}^{n_{\text{rea}}} w_{ik}(\mathbf{p})} - g_{\text{true},k} \right)^2$$

Simulation size: 50 M stamps for each set, 100 M stamps for validation.  
Probably more in future.

# Illustration with VIS simulations (simple: single Sérsic stamps)

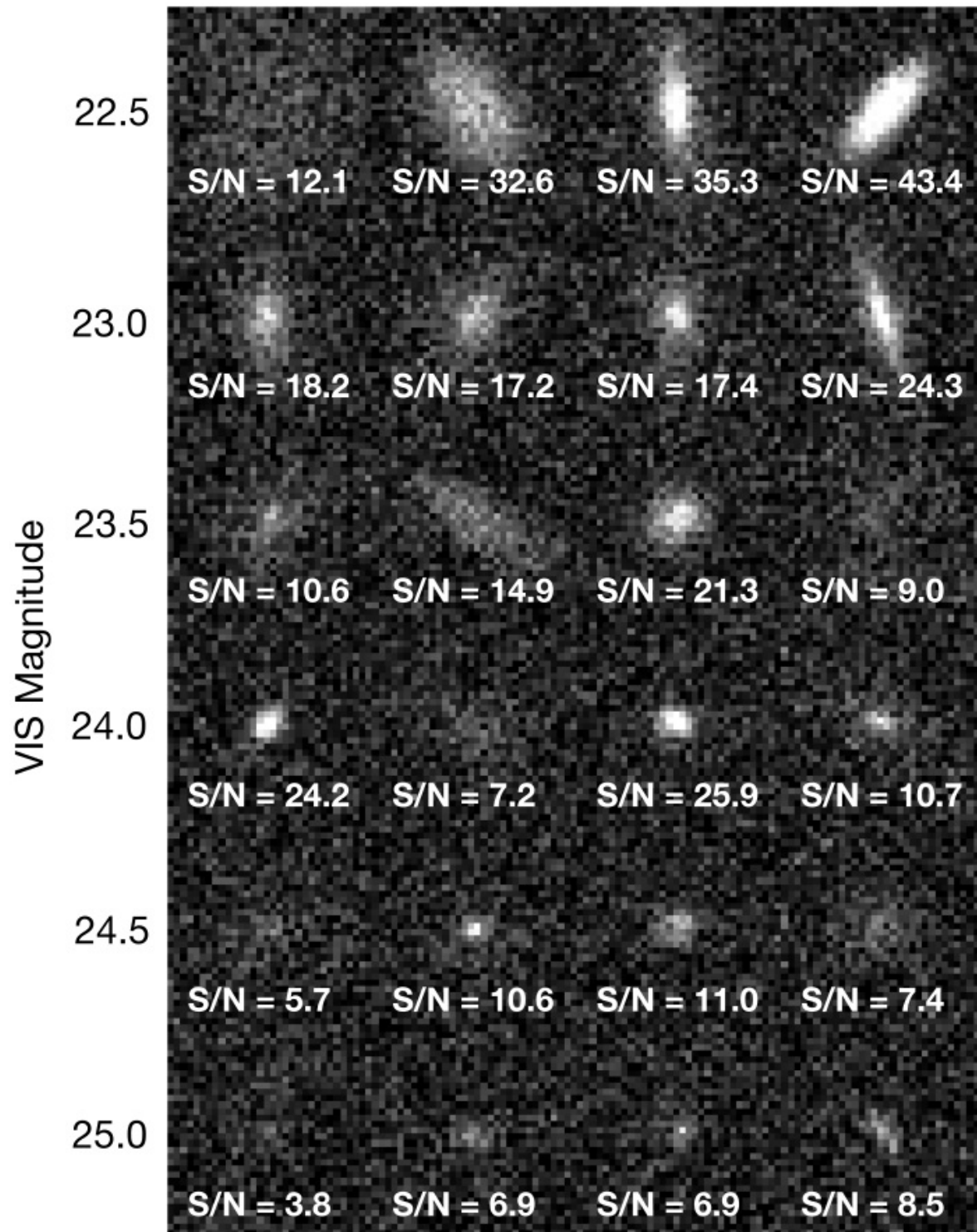


Galaxy parameters from GEMS (Rix et al. 2004), VIS zero-point empirically adjusted to meet S/N 10 at Mag 24.5



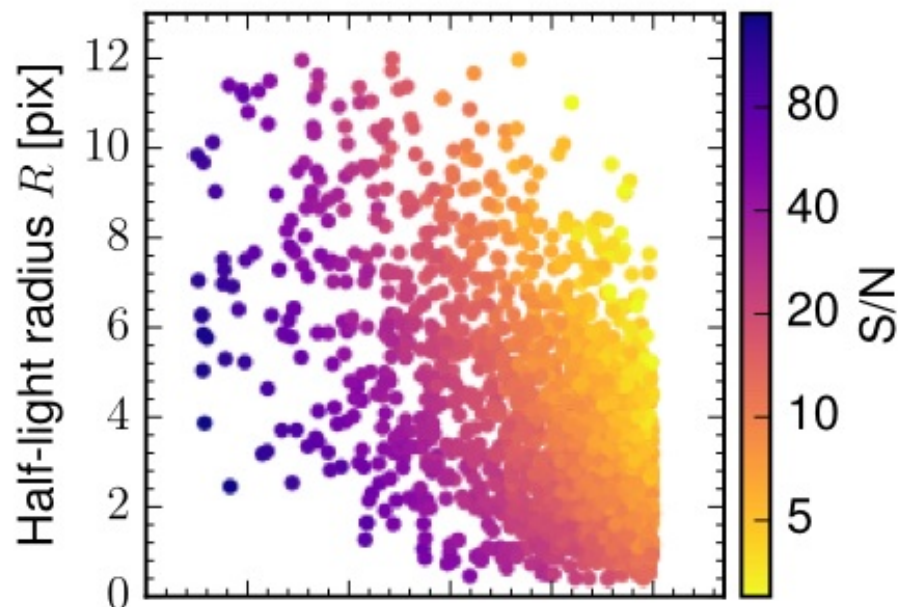
Euclid-like PSF (simple GalSim generation), shown on a grid of 0.02'' per pixel with a logarithmic grayscale.





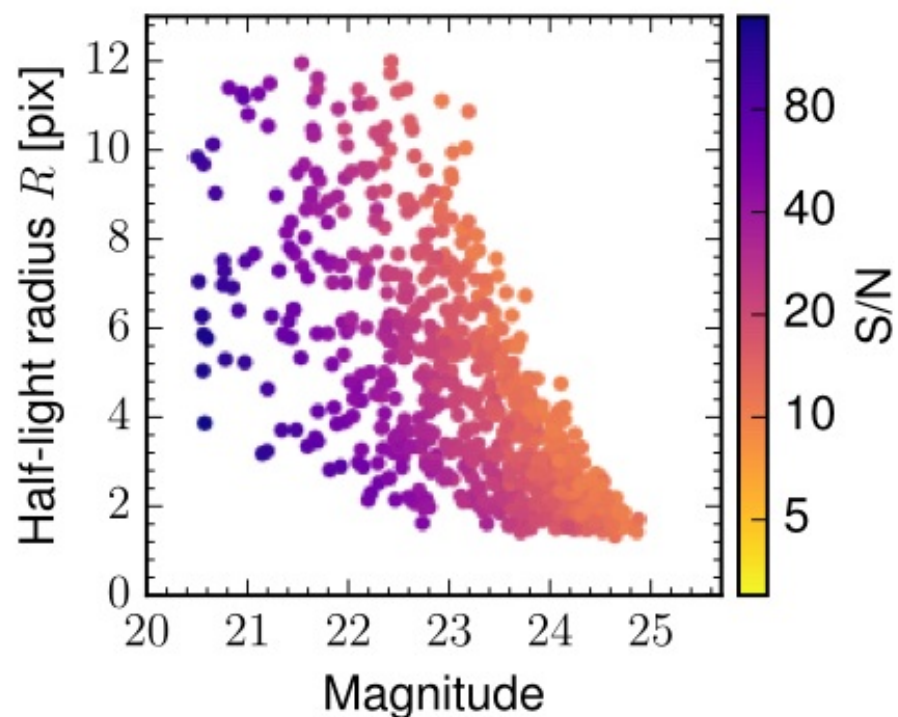
# Mimicking a galaxy selection function

Simulation source catalog:



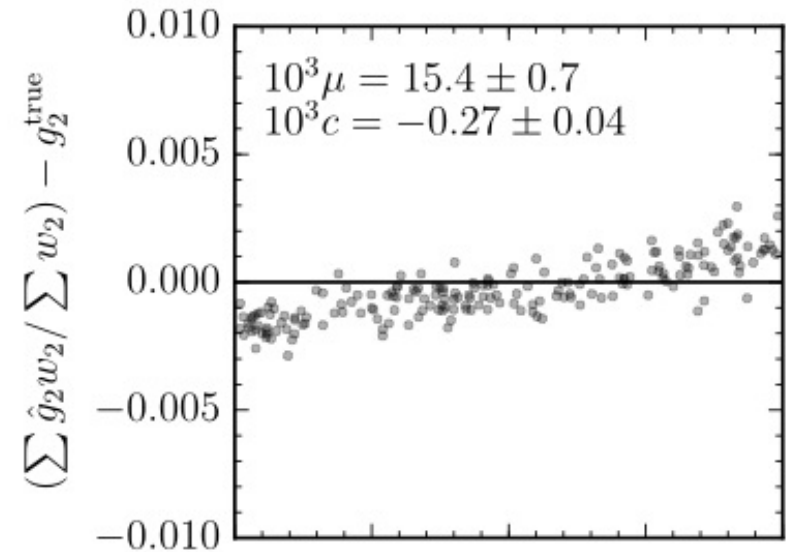
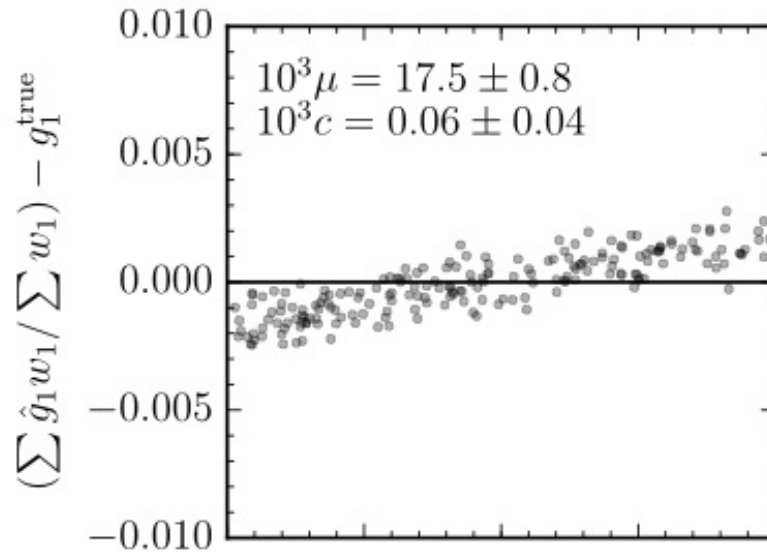
Selection of *measured*  $S/N > 10$ ,  
and *measured* radius  $> 1.5$  pixel:

Leads to shear biases, as  
(1) the measured quantities on  
which the selection is made  
correlate with shear, and  
(2) a shear estimation method is  
sensitive to the population.

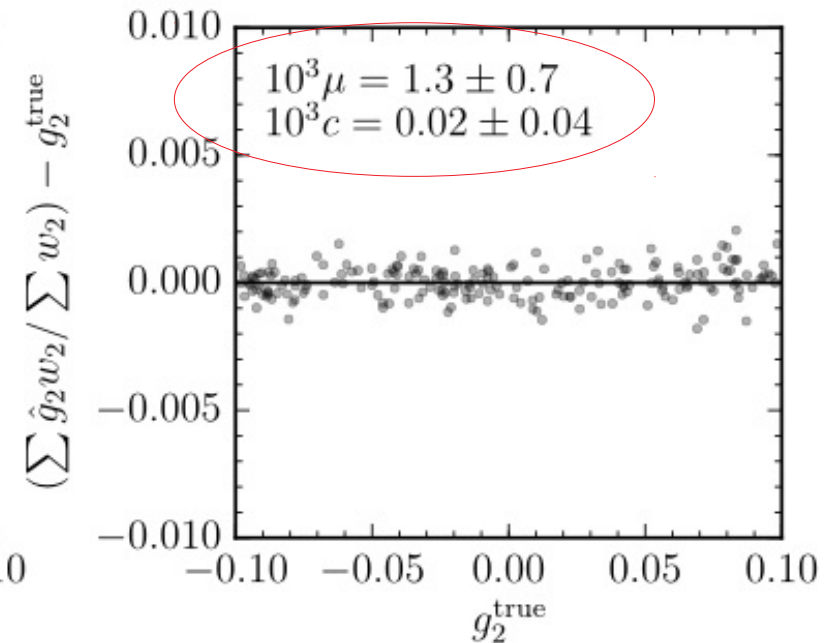
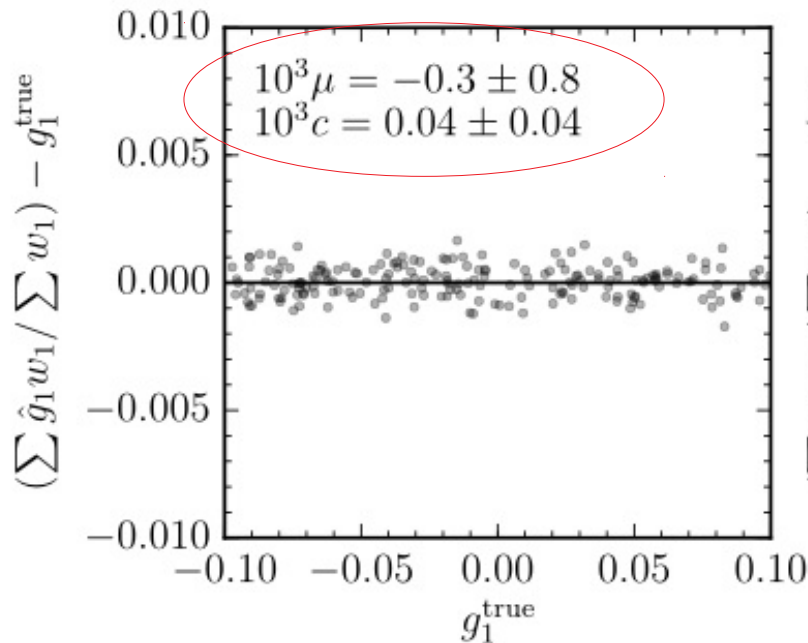


# Weights trained with selection fct cancel-out selection biases

Without taking into account the selection



Training the weight estimator with the given selection function



Simplified Euclid-like simulations

# Tests with Great3 simulations

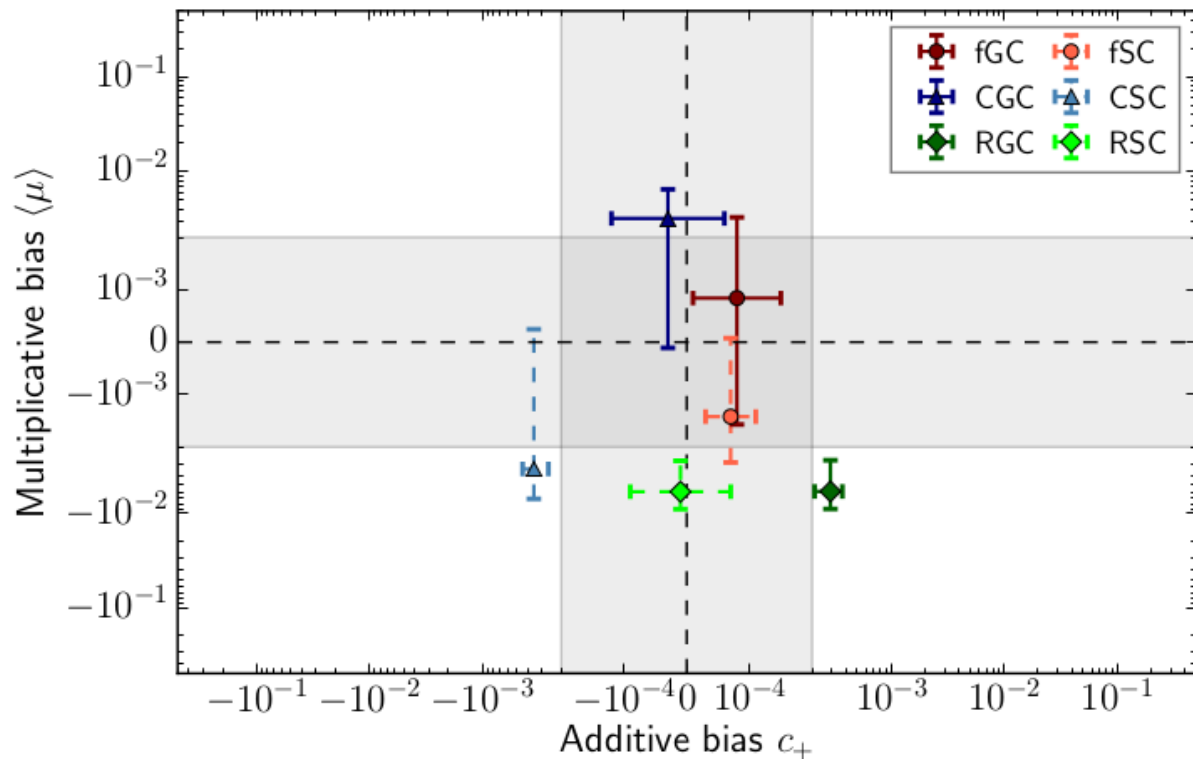
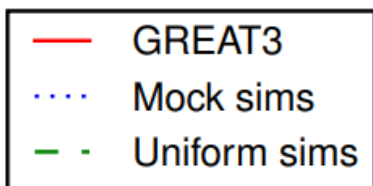


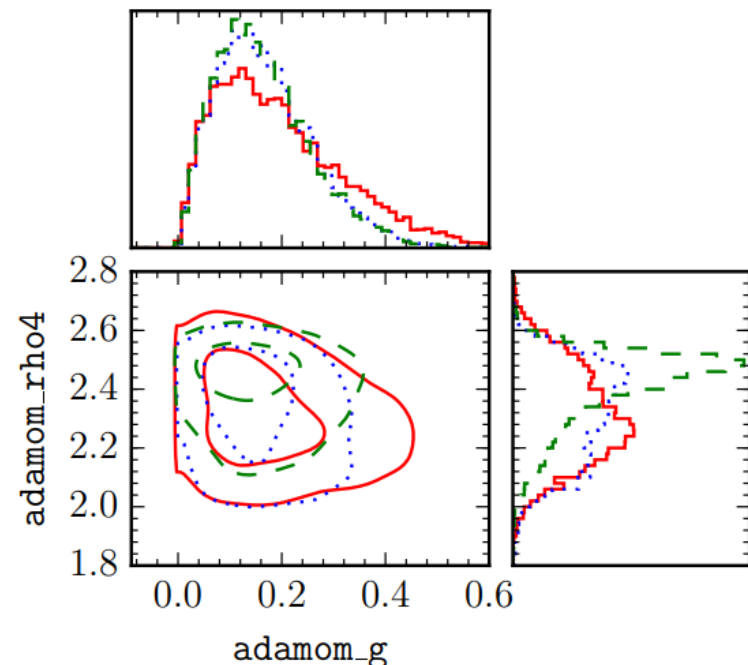
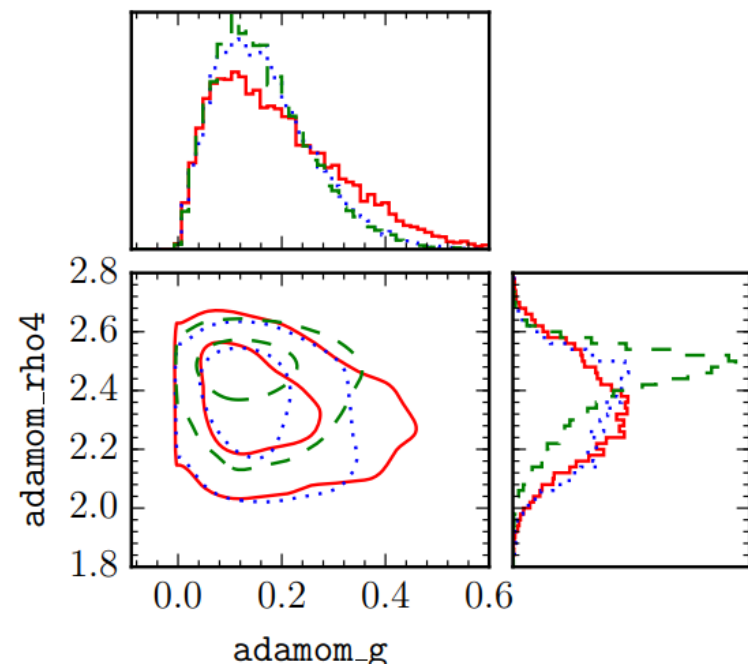
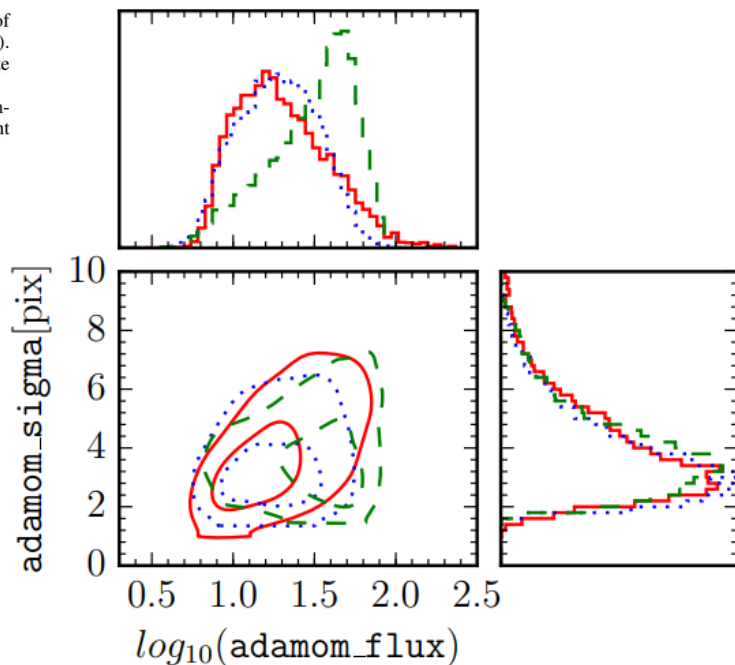
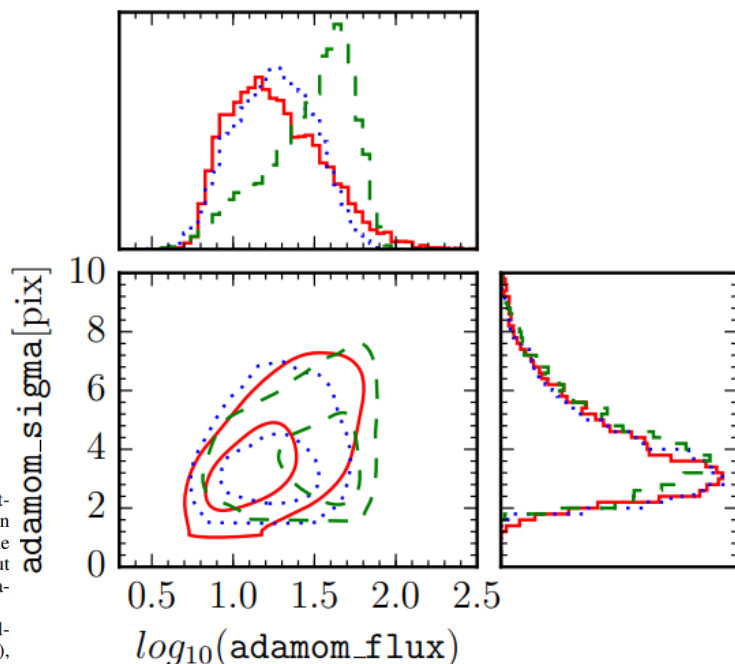
**Fig. 24.** Multiplicative bias  $\mu$  averaged over the components 1 and 2, against the additive bias  $c_+$  defined in the coordinate system of the PSF anisotropy. This figure can be directly compared with Fig. 17 of the GREAT3 result paper (Mandelbaum et al. 2015). Space branches are shown with dashed error bars. Note that the axes are linear within the the gray-shaded region, and logarithmic outside.

- **C**: GREAT3 Control branch (2 Sersic profiles)
- **R**: Realistic galaxy shapes from HST postage stamps
- **f**: Fiducial set (1 Sersic)
- **S**: Space-based resolution
- **G**: Ground-based resolution
- Training with simple single-Sersic galaxies
- Recovery close to requirements  
→ **Low sensitivity** to exact galaxy properties!
- Larger simulations needed to really test against requirements



## CSC

Subfield 045



`adamom_flux` corresponds to the total source flux of the best-fit elliptical Gaussian profile (`ShapeData.moments_amp` in `GalSim`), expressed in ADU. This is a biased estimate of the flux of any realistic (i.e., non-Gaussian) galaxy profile, but such biases have no direct consequences for ML input features.

`adamom_g1` and `adamom_g2` are components of the observed ellipticity (`ShapeData.observed_shape.g1/2` in `GalSim`), which would correspond, for a simple elliptical Gaussian profile and without PSF, noise, and pixellation, to the ellipticity defined in Sect. 2 as an estimator for shear.

`adamom_sigma` gives a measurement of the radial extension of the profile, in units of pixels (`ShapeData.moments_sigma`). In the case of a circular Gaussian profile, it would estimate its standard deviation.

`adamom_rho4` gives a weighted radial fourth moment of the image, measuring the concentration, i.e., a kurtosis, of the light profile (`ShapeData.moments_rho4` in `GalSim`).

## RSC

Subfield 194

## 3. Using HST data for the Euclid shape calibration

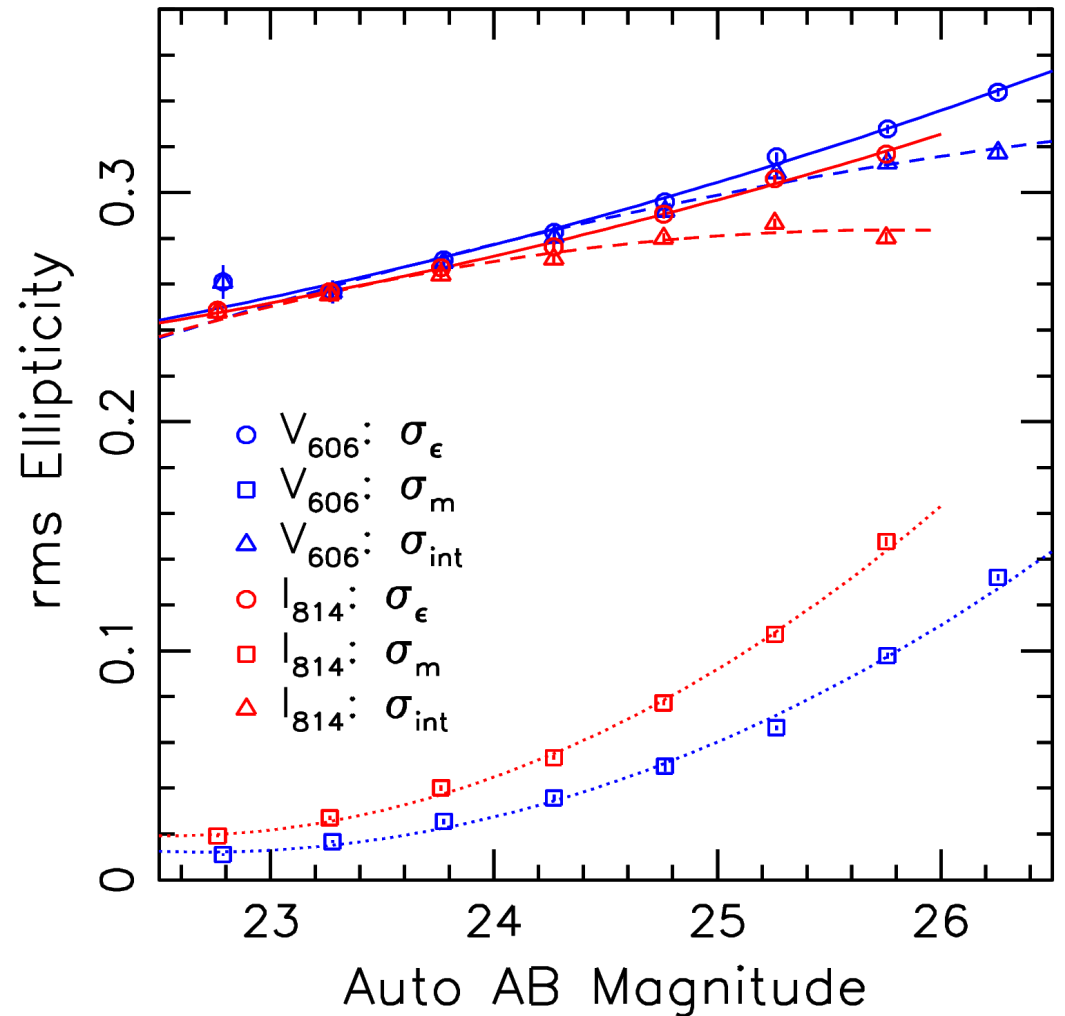
- **Higher resolution:** 0.1" compared to 0.2" for Euclid
- **Multiple filters** → Spatially resolved colours
- Deeper than Euclid-Wide, but much smaller sky coverage

### **Use HST images of galaxies that are representative for the galaxies observed by Euclid to...**

- Account for the impact of colour gradients → Presentation by Xinzong Er
- Use HST galaxies as input for Euclid image simulations (galsim)
- Obtain priors for distributions of galaxy shape parameters (will be updated using Euclid-Deep data)
- Study the impact of galaxies beyond the Euclid detection limit on Euclid shape measurements

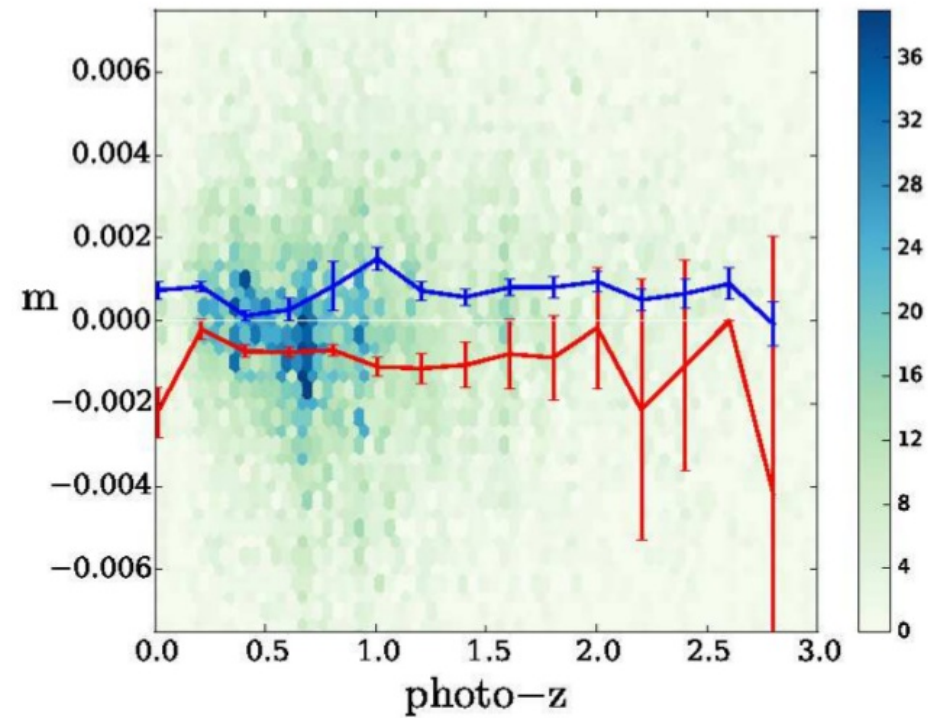
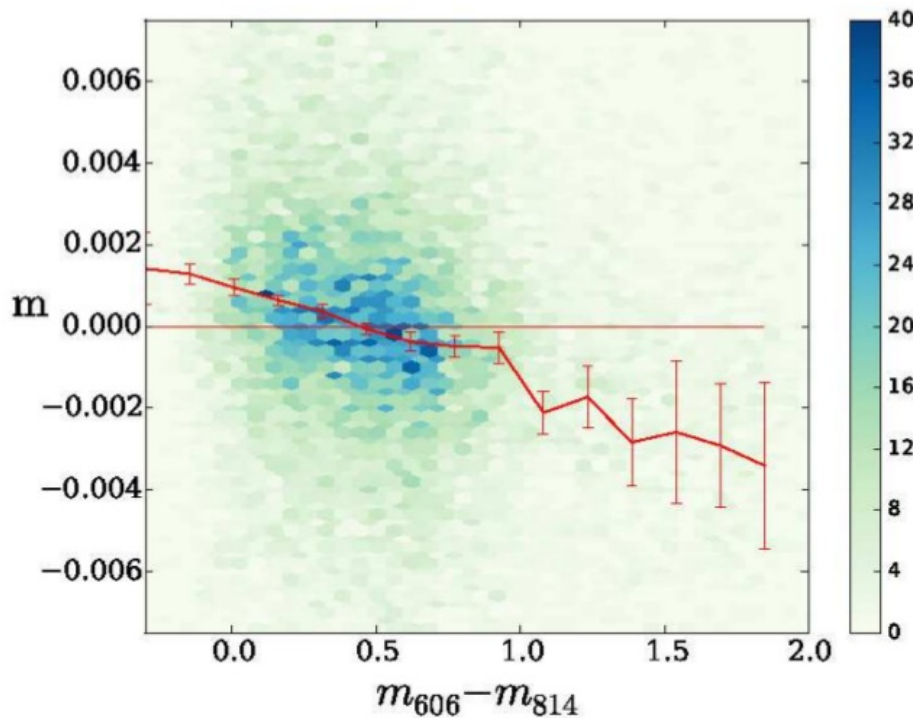
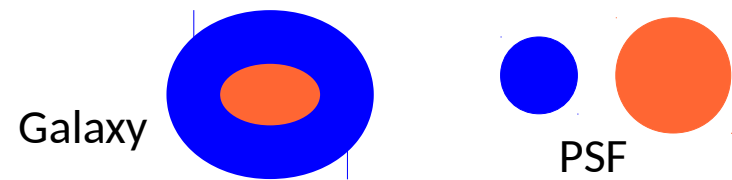
# Galaxy shape distribution

- Measurement of the **intrinsic galaxy ellipticity dispersion** based on our initial reduction of CANDELS V606W+F814W images
- For the first time showed that this is clearly magnitude and band-pass dependent



# Derive a statistical correction for shape measurement biases induced by colour gradients

Er, Hoekstra, Schrabback, et al. 2018,  
MNRAS, 476, 5645



- Need a correction as function of redshift and galaxy properties
- Plan to revise the analysis using more & deeper HST stacks (pipeline updates ongoing, lead: Marggraf) & actual Euclid shape measurement techniques
- Will obtain missing requirement flow down (SWG) via funding from the EU H2020 EWC programme (PI: Kitching)



# Using HST images as galsim input

- Need to degrade from HST to target (Euclid) resolution. In addition: galaxies need to be sheared! Does not commute!
- First deconvolve for the HST PSF, then shear, then convolve to the target PSF size
- Works well if the target resolution is significantly worse than the input
- Has been pioneered by R. Mandelbaum in SHERA and further developed in galsim (Rowe et al. 2015)
- **Things to keep in mind:**
  - Shearing leads to correlated noise → Add anticorrelated noise to whiten the total noise → Final image will be more noisy
  - Need to properly account for neighbours, e.g. perform object detection and selection with correct resolution to identify the HST pixels belonging to one “galaxy” defined at lower resolution (see e.g. Mandelbaum et al. 2018)
  - Need a good HST PSF model

# Validation of PSF Models for HST and Other Space-Based Observations

Bryan R. Gillis<sup>1\*</sup>, Tim Schrabbach<sup>2</sup>, Ole Marggraf<sup>2</sup>,  
Rachel Mandelbaum<sup>3</sup>, Richard Massey<sup>4,5</sup>, Jason Rhodes<sup>6,7</sup>, Andy Taylor<sup>1</sup>

<sup>1</sup>*Institute for Astronomy, University of Edinburgh, Royal Observatory Edinburgh, Edinburgh, EH9 3HJ, United Kingdom.*

<sup>2</sup>*Argelander Institute for Astronomy, University of Bonn, Auf dem Hügel 71, 53121 Bonn, Germany*

<sup>3</sup>*McWilliams Center for Cosmology, Department of Physics, Carnegie Mellon University, Pittsburgh, PA 15213, USA,*

<sup>4</sup>*Centre for Extragalactic Astronomy, Department of Physics, Durham University, Durham DH1 3LE, U.K.,*

<sup>5</sup>*Institute for Computational Cosmology, Durham University, South Road, Durham DH1 3LE, U.K.,*

<sup>6</sup>*Jet Propulsion Laboratory, California Institute of Technology, 4800 Oak Grove Dr., Pasadena, CA 91109, USA,*

<sup>7</sup>*California Institute of Technology, 1200 E. California Blvd., CA 91125, USA*

17 Jun 2019

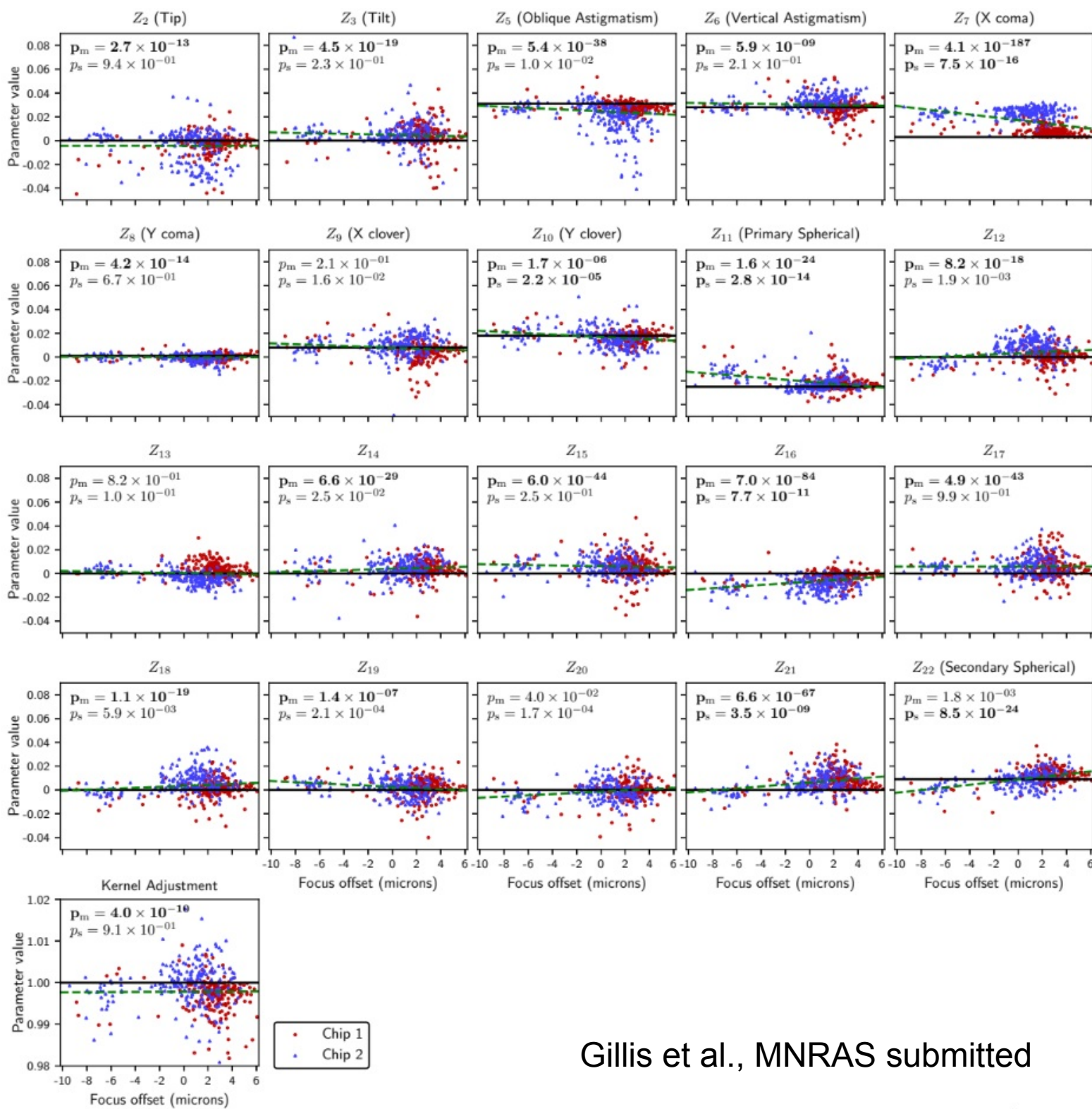


## ABSTRACT

Forthcoming space-based observations will require high-quality point-spread function (PSF) models for weak gravitational lensing measurements. One approach to generating these models is using a wavefront model based on the known telescope optics. We present an empirical framework for validating such models to confirm that they match the actual PSF to within requirements by comparing the models to the observed light distributions of isolated stars. We apply this framework to Tiny Tim, the standard tool for generating model PSFs for the *Hubble Space Telescope* (HST), testing its models against images taken by HST's Advanced Camera for Surveys in the Wide Field Channel. We show that Tiny Tim's models, in the default configuration, differ significantly from the observed PSFs, most notably in their sizes. We find that the quality of Tiny Tim PSFs can be improved through fitting the full set of Zernike polynomial coefficients which characterise the optics, to the point where the practical significance of the difference between model and observed PSFs is negligible for most use cases, resulting in additive and multiplicative biases both of order  $\sim 4 \times 10^{-4}$ . We also show that most of this improvement can be retained through using an updated set of Zernike coefficients, which we provide.

## Key words:

gravitational lensing: weak; methods: data analysis



# 4. Impact of faint galaxies

## ***Euclid* preparation: IV. Impact of undetected galaxies on weak-lensing shear measurements** ★

*Euclid* Collaboration, N. Martinet<sup>1,2</sup>, T. Schrabback<sup>1</sup>, H. Hoekstra<sup>3</sup>, M. Tewes<sup>1</sup>, R. Herbonnet<sup>4</sup>, P. Schneider<sup>1</sup>, B. Hernandez-Martin<sup>1</sup>, A.N. Taylor<sup>5</sup>, J. Brinchmann<sup>3,6</sup>, C.S. Carvalho<sup>7</sup>, M. Castellano<sup>8</sup>, G. Congedo<sup>5</sup>, B.R. Gillis<sup>5</sup>, E. Jullo<sup>2</sup>, M. Kümmel<sup>9</sup>, S. Ligi<sup>10</sup>, P.B. Lilje<sup>11</sup>, C. Padilla<sup>12</sup>, D. Paris<sup>8</sup>, J.A. Peacock<sup>5</sup>, S. Pilo<sup>8</sup>, A. Pujol<sup>13,14</sup>, D. Scott<sup>15</sup>, R. Toledo-Moreo<sup>16</sup>



<sup>1</sup> Argelander-Institut für Astronomie, Universität Bonn, Auf dem Hügel 71, 53121 Bonn, Germany

<sup>2</sup> Aix-Marseille Univ, CNRS, CNES, LAM, Marseille, France

<sup>3</sup> Leiden Observatory, Leiden University, Niels Bohrweg 2, 2333 CA Leiden, the Netherlands

<sup>4</sup> Department of Physics and Astronomy, Stony Brook University, Stony Brook, NY 11794, USA

<sup>5</sup> Institute for Astronomy, University of Edinburgh, Royal Observatory, Blackford Hill, Edinburgh EH9 3HJ, UK

<sup>6</sup> Instituto de Astrofísica e Ciências do Espaço, Universidade do Porto, CAUP, Rua das Estrelas, PT4150-762 Porto, Portugal

<sup>7</sup> Instituto de Astrofísica e Ciências do Espaço, Faculdade de Ciências, Universidade de Lisboa, Tapada da Ajuda, PT-1349-018 Lisboa, Portugal

<sup>8</sup> INAF-Osservatorio Astronomico di Roma, via Frascati 33, I-00078 Monteporzio Catone, Italy

<sup>9</sup> Universitäts-Sternwarte München, Fakultät für Physik, Ludwig-Maximilians-Universität München, Scheinerstrasse 1, 81679 München, Germany

<sup>10</sup> INAF-Osservatorio Astrofisico di Torino, via Osservatorio 20, 10025 Pino Torinese (TO), Italy

<sup>11</sup> Institute of Theoretical Astrophysics, University of Oslo, P.O. Box 1029 Blindern, N-0315 Oslo, Norway

<sup>12</sup> Institut de Física d'Altes Energies IFAE, 08193 Bellaterra, Barcelona, Spain

<sup>13</sup> Université Paris Diderot, AIM, Sorbonne Paris Cité, CEA, CNRS F-91191 Gif-sur-Yvette Cedex, France

<sup>14</sup> IRFU, CEA, Université Paris-Saclay F-91191 Gif-sur-Yvette Cedex, France

<sup>15</sup> Department of Physics and Astronomy, University of British Columbia, Vancouver, BC V6T 1Z1, Canada

<sup>16</sup> Depto. de Electrónica y Tecnología de Computadoras Universidad Politécnica de Cartagena, 30202, Cartagena, Spain  
e-mail: nicolas.martinet@lam.fr

Preprint online version: July 3, 2019

### ABSTRACT

In modern weak-lensing surveys, the common approach to correct for residual systematic biases in the shear is to calibrate shape measurement algorithms using simulations. These simulations must fully capture the complexity of the observations to avoid introducing any additional bias. In this paper we study the importance of faint galaxies below the observational detection limit of a survey. We simulate simplified *Euclid* VIS images including and excluding this faint population, and measure the shift in the multiplicative shear bias between the two sets of simulations. We measure the shear with three different algorithms: a moment-based approach, model fitting, and machine learning. We find that for all methods, a spatially uniform random distribution of faint galaxies introduces a shear multiplicative bias of the order of a few times  $10^{-3}$ . This value increases to the order of  $10^{-2}$  when including the clustering of the faint galaxies, as measured in the *Hubble* Space Telescope Ultra-Deep Field. The magnification of the faint background galaxies due to the brighter galaxies along the line of sight is found to have a negligible impact on the multiplicative bias. We conclude that the undetected galaxies must be included in the calibration simulations with proper clustering properties down to magnitude 28 in order to reach a residual uncertainty on the multiplicative shear bias calibration of a few times  $10^{-4}$ , in line with the  $2 \times 10^{-3}$  total accuracy budget required by the scientific objectives of the *Euclid* survey. We propose two complementary methods for including faint galaxy clustering in the calibration simulations.

**Key words.** gravitational lensing: weak – cosmology: observations – surveys

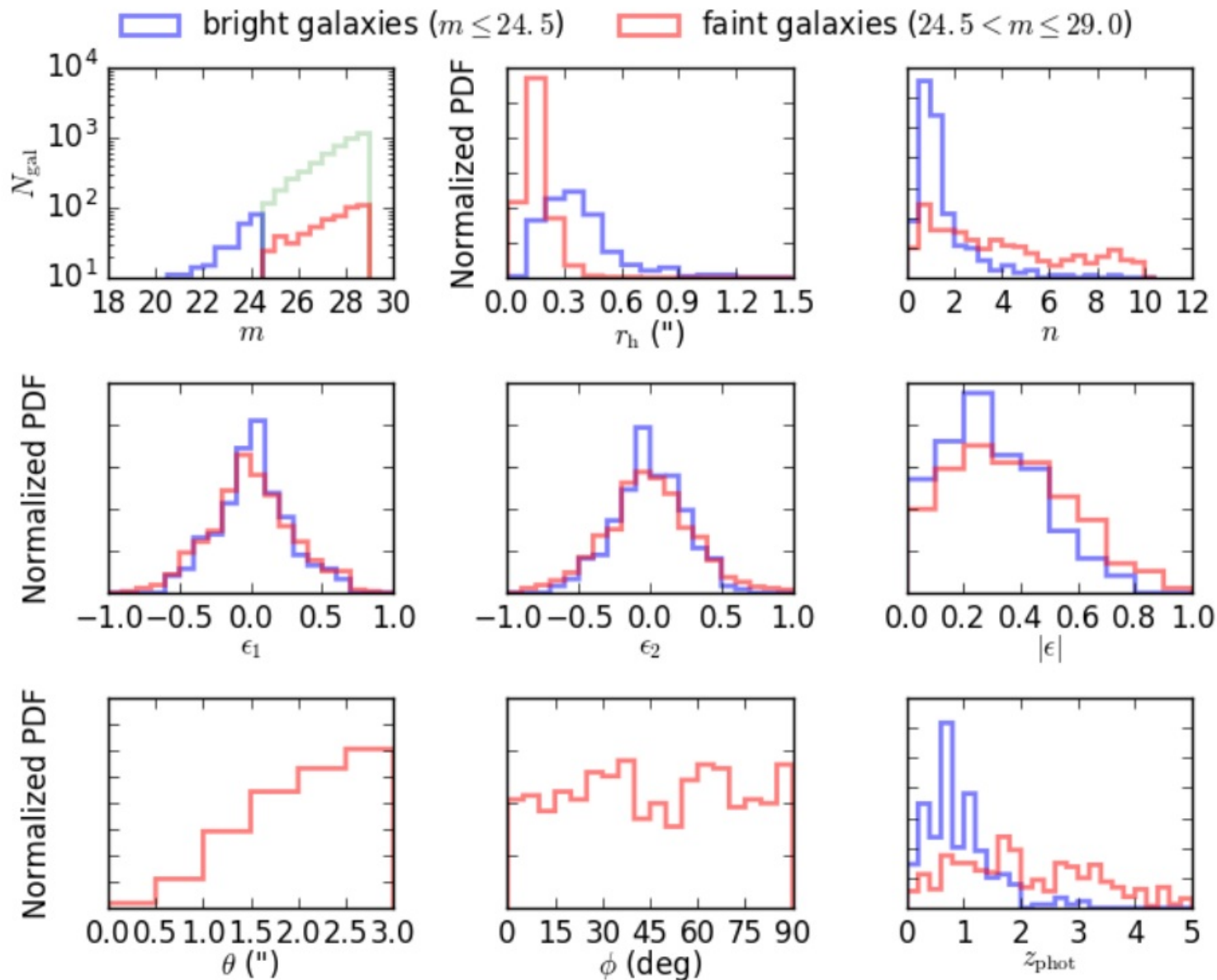


**Fig. 4.** Distributions of galaxy parameters measured with SExtractor in the UDF. The panels show histograms of galaxy magnitudes ( $m$ , *top left*), half-light radius ( $r_h$ , *top middle*), Sérsic index ( $n$ , *top right*), ellipticity components ( $\epsilon_1$ ,  $\epsilon_2$ , *middle left*, *middle middle*), ellipticity modulus ( $|\epsilon|$ , *middle right*), distance to nearest bright galaxy ( $\theta$ , *bottom left*), faint galaxy position angle relative to the nearest bright galaxy major axis ( $\phi$ , *bottom middle*), and photometric redshifts ( $z_{\text{phot}}$ , *bottom right*). Blue histograms correspond to bright galaxies ( $m \leq 24.5$ ) and red to faint galaxies ( $24.5 < m \leq 29$ ) lying within  $3''$  of a bright one. The green histogram in the top left panel shows the magnitude distribution of all faint galaxies up to  $m = 29$ .

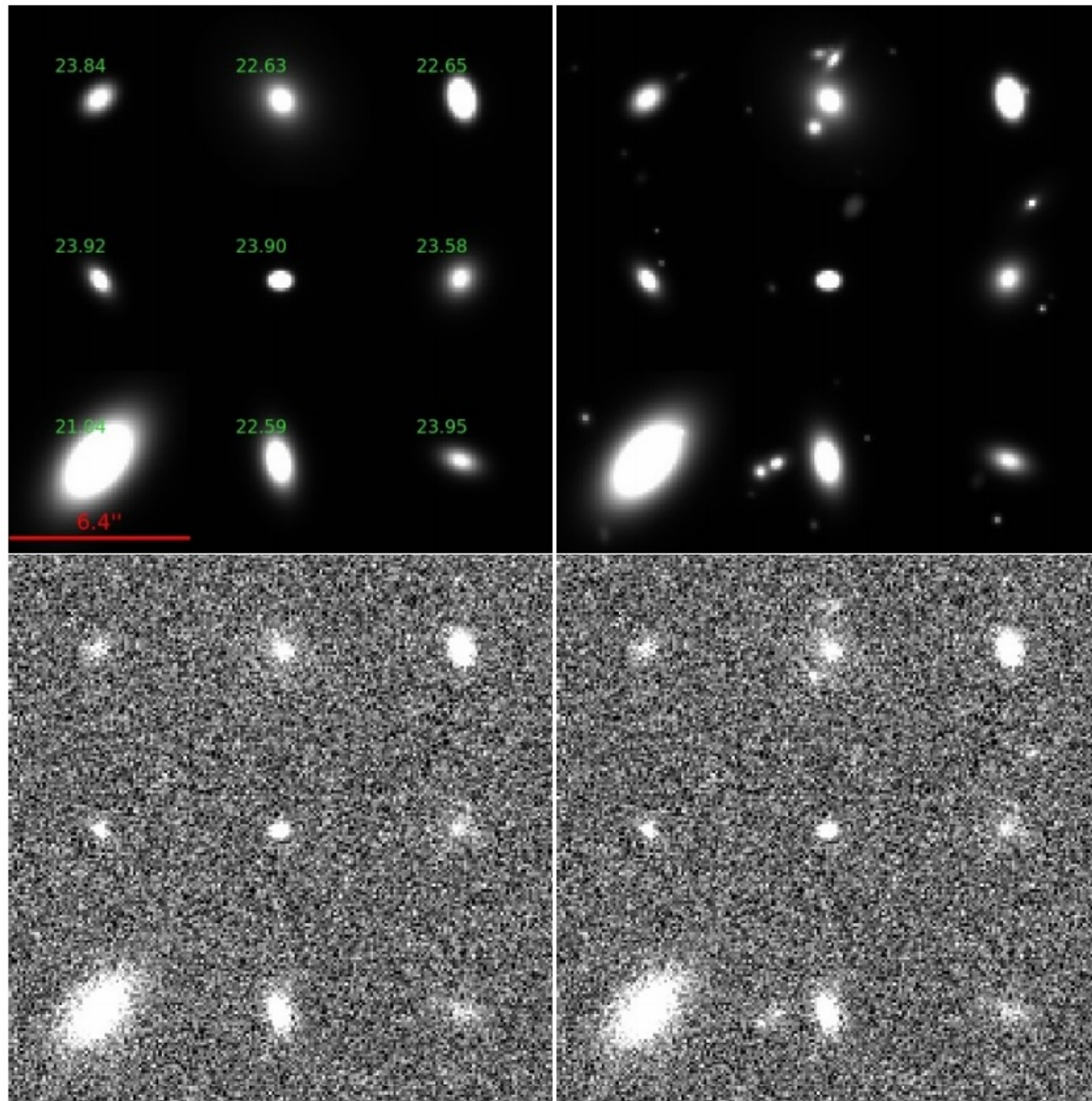
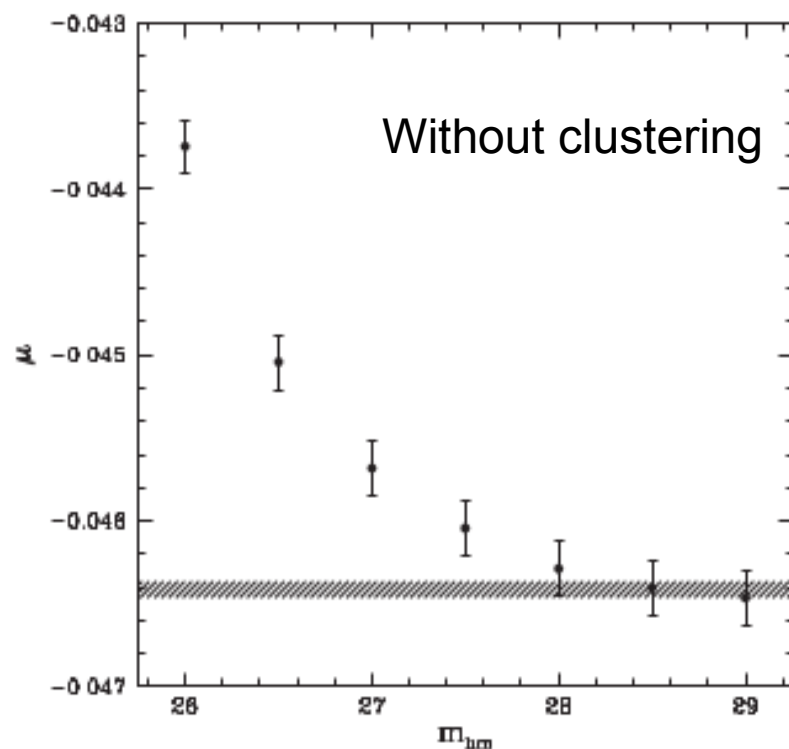


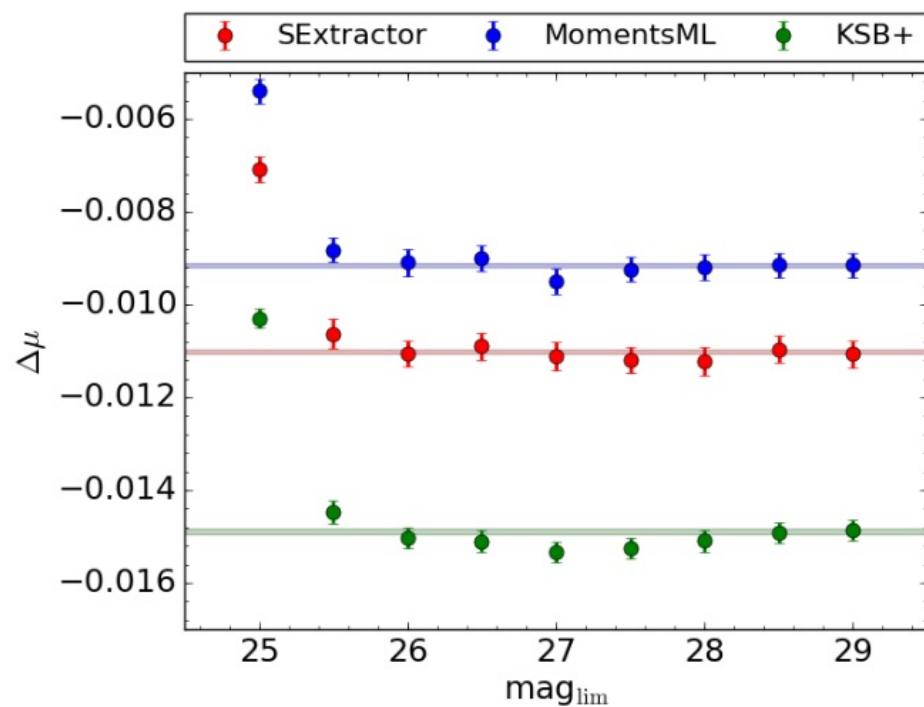
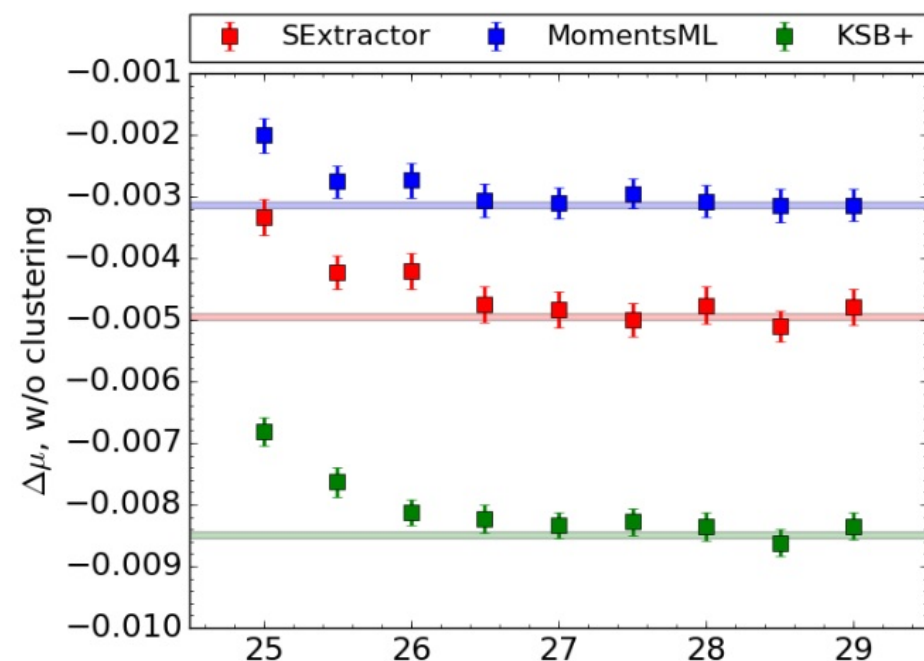
**Fig. 6.** Image simulations, with bright galaxies on a grid (*left*), and with the faint galaxies down to magnitude 29 added, including clustering properties (*right*). The *upper panel* shows noiseless simulations and the *bottom* one simulations with realistic Gaussian noise. This sub-image presents nine tiles of  $6''.4 \times 6''.4$  each. The scale is given by the red line in the upper left panel. The numbers in the same panel correspond to the magnitudes of the bright galaxies. The two right panels are populated with an identical set of 30 faint galaxies.

# 4. Impact of faint galaxies



Hoekstra et al. 2017, MNRAS 468, 3295

- Bias exceeds Euclid requirements by almost an order of magnitude if ignored
- Clearly method dependent
- Simplified faint source clustering now incorporated into SC456
- Need to study galaxies at least to  $\text{VIS} \sim 27$ .  $\rightarrow$  More HST data+Euclid-Deep



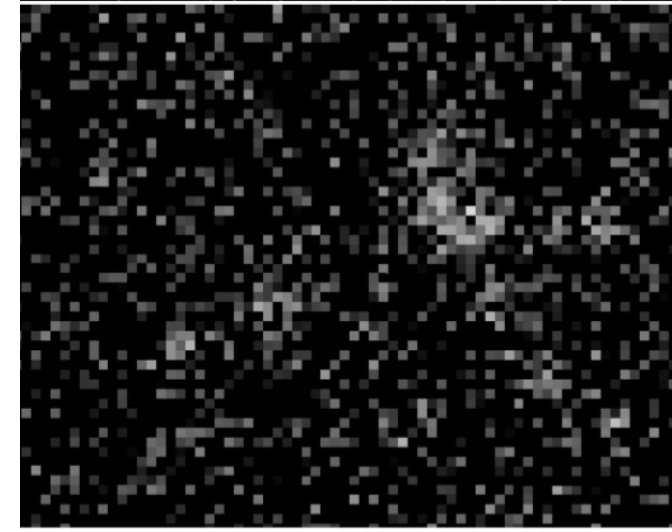
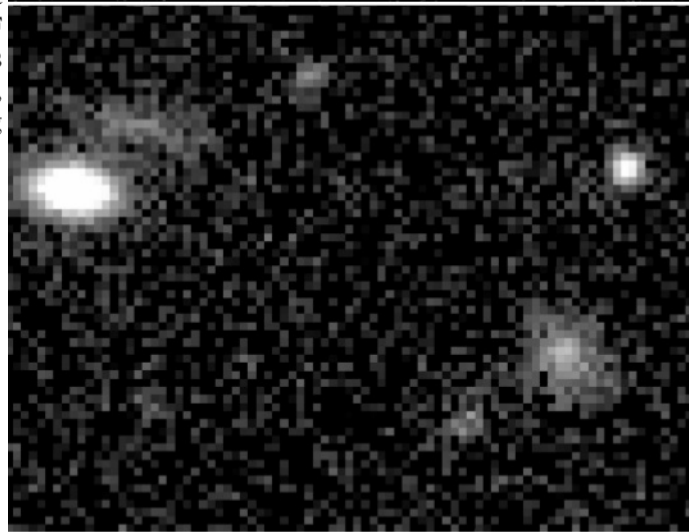
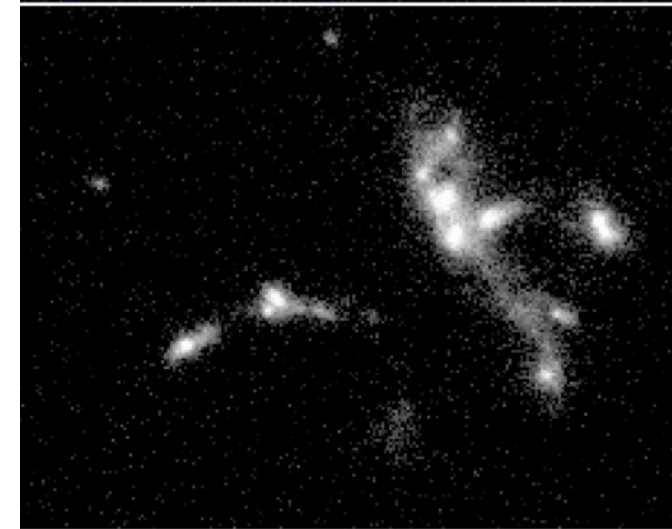
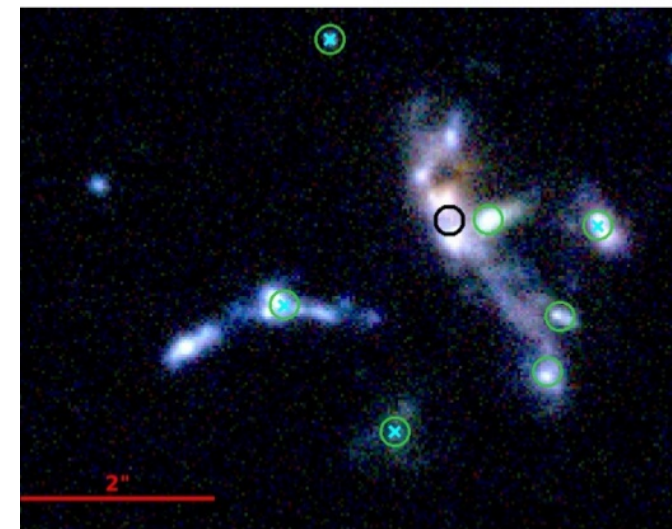
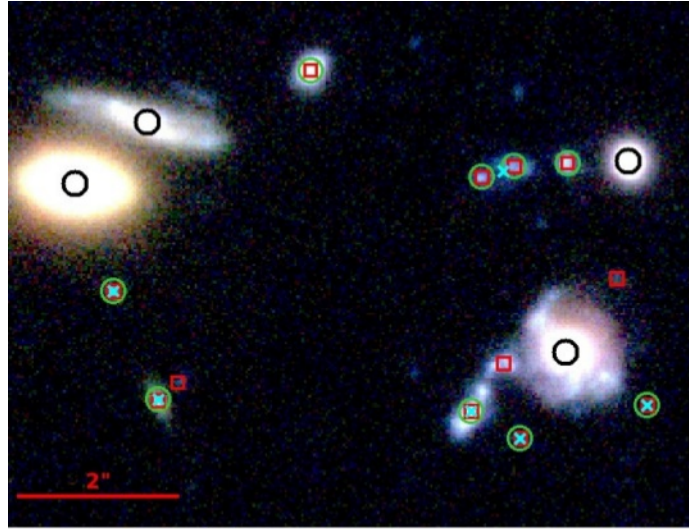


**Table 2.** Shifts in the shear multiplicative bias due to the faint galaxies with density and clustering measured on the UDF data for various deblending strategies. Weak deblending refers to (DEBLEND\_NTHRESH, DEBLEND\_MINCONT) values of (8, 0.05), fiducial deblending to (16, 0.01), and strong deblending to (32, 0.001)

	weak deblending	fiducial deblending	strong deblending
w/o clustering			
$\Delta\mu^{\text{SEx}} \times 10^3$	$-4.91 \pm 0.28$	$-4.79 \pm 0.30$	$-8.27 \pm 0.28$
$\Delta\mu^{\text{ML}} \times 10^3$	$-2.63 \pm 0.27$	$-3.14 \pm 0.27$	$-6.50 \pm 0.28$
$\Delta\mu^{\text{KSB}} \times 10^3$	$-8.20 \pm 0.22$	$-8.35 \pm 0.21$	$-11.30 \pm 0.23$
with clustering			
$\Delta\mu^{\text{SEx}} \times 10^3$	$-3.99 \pm 0.31$	$-11.06 \pm 0.29$	$-36.98 \pm 0.35$
$\Delta\mu^{\text{ML}} \times 10^3$	$-2.20 \pm 0.29$	$-9.15 \pm 0.27$	$-35.29 \pm 0.30$
$\Delta\mu^{\text{KSB}} \times 10^3$	$-7.16 \pm 0.21$	$-14.87 \pm 0.22$	$-43.26 \pm 0.26$



## 5. Simulating cluster fields

- Cluster fields experience stronger shear and increased blending
- Relevant for cluster science and also contributes to cosmic shear
- Need to properly account for these effects
- Initial study done by Beatriz Hernandez Martin for our KSB+ implementation

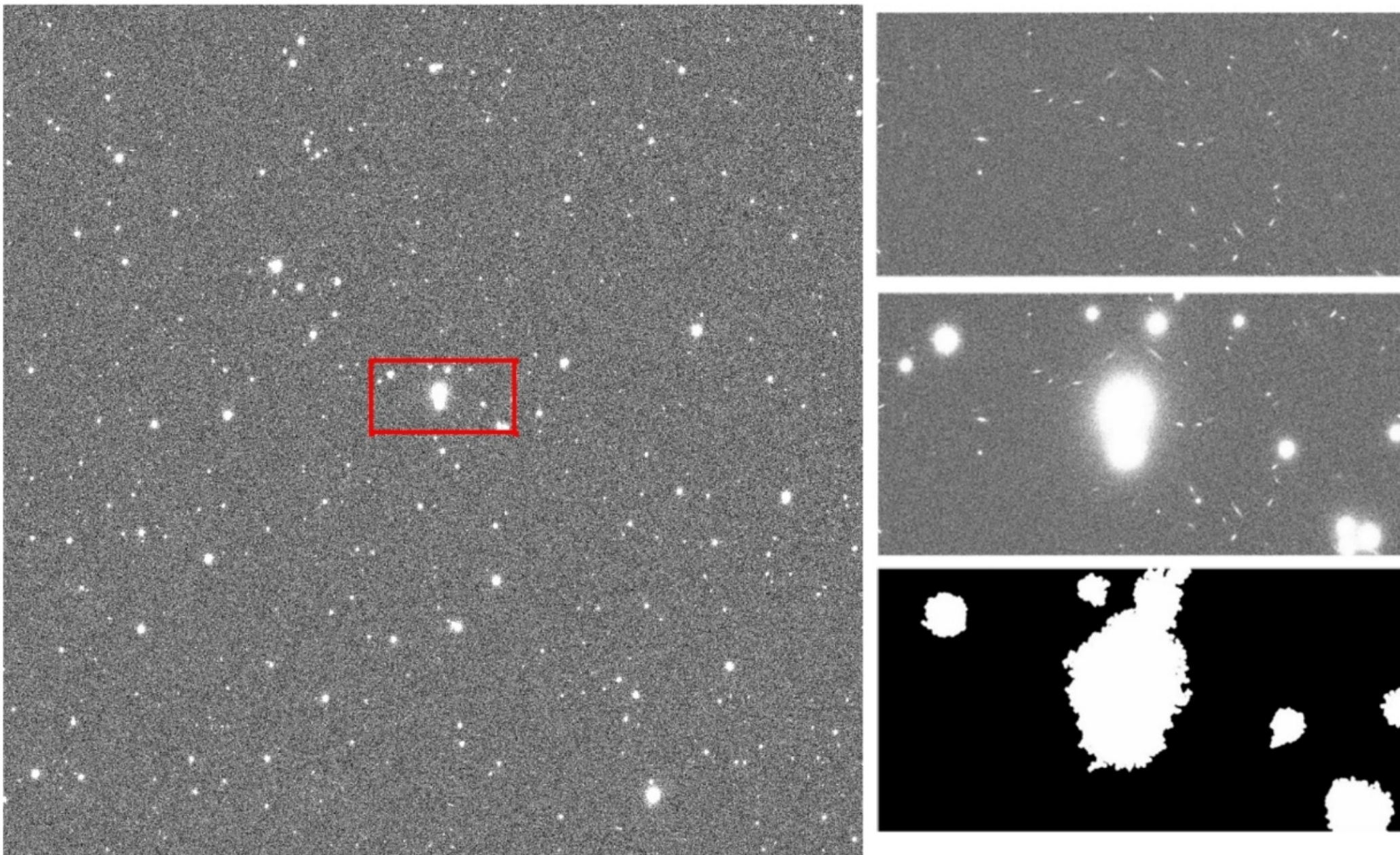
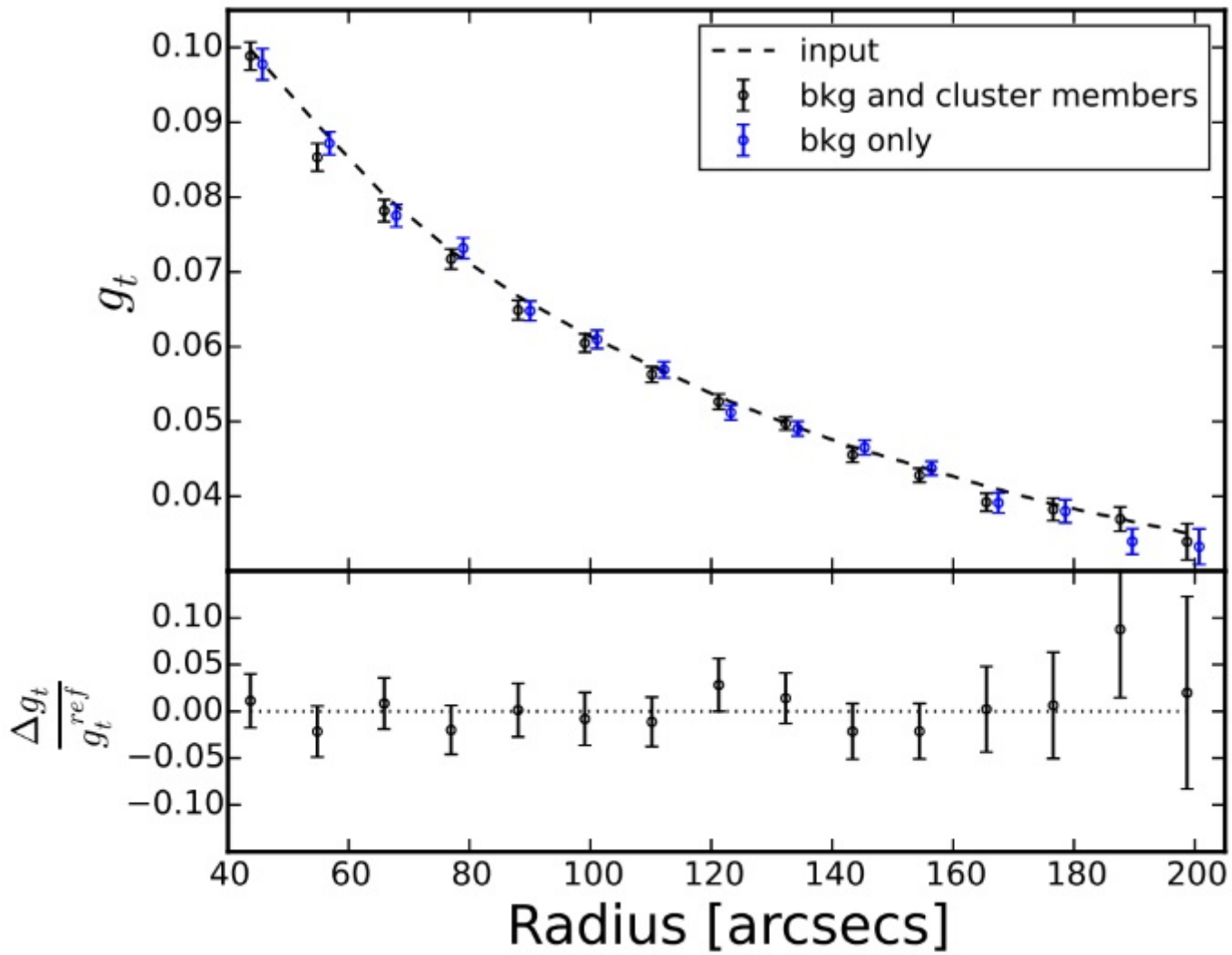


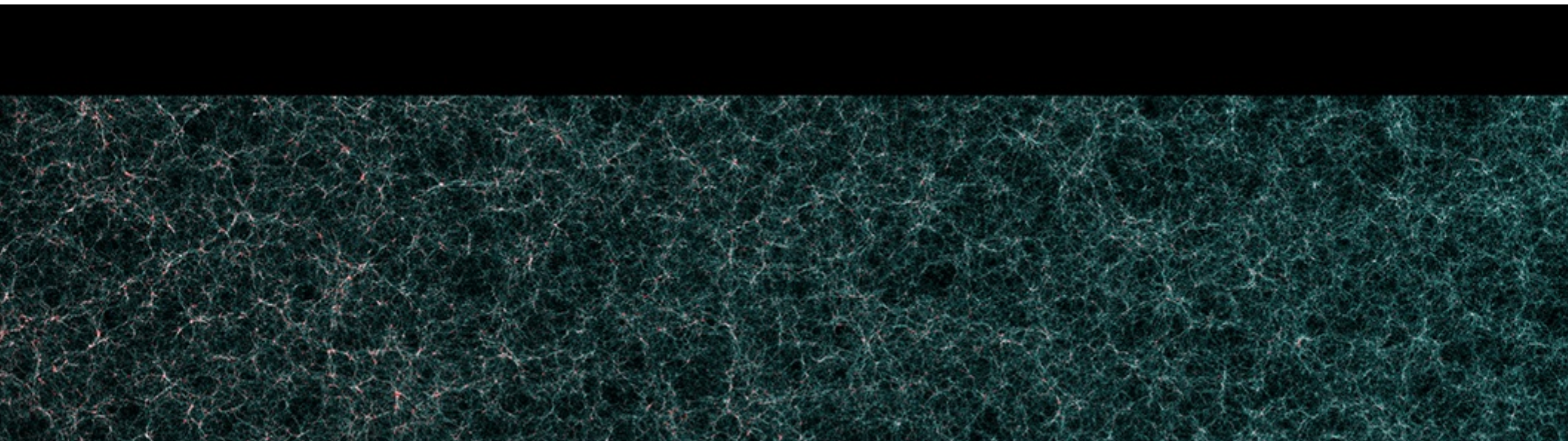
**Fig. 9.** Example image of a simulated cluster at  $z = 0.29$ . A cut-out of the full image, shown in red, can be seen in the right for the simulations with background galaxies only (top), with added cluster members (middle) and showing the mask used to remove bright objects (bottom). The full image and cut outs spans  $300'' \times 300''$  and  $50'' \times 25''$ , respectively.



## 6. OU-SIM simulations

- Extensive simulation efforts within the Euclid OU-SIM
- Simulating Euclid+ground-based observations in all bands, using mock catalogs from the Euclid flagship simulations as input
- Based on galsim, currently using parametric galaxy models
- Including simulation of instrument effects and defects (e.g. hot pixels, cosmic rays, ghosts, etc.)
- Euclid pipeline is run on these simulations. Should provide residuals, whose impact on shape measurements needs to be calibrated.

<https://sci.esa.int/web/euclid/-/59348-euclid-flagship-mock-galaxy-catalogue>



## 7. Summary

- Weak lensing simulations are essential in order to train and calibrate shape measurement methods
- The simulations must provide a good approximation of the truth, thus it is useful to base the inputs on real observations, either directly using HST images as input or trying to emulate HST observations
- It is preferable to use shape measurement methods whose biases show only a weak dependence on the details of the simulations
- Also need to calibrate impact of residual detector effects and image artifacts